ACS APPLIED POLYMER MATERIALS

pubs.acs.org/acsapm Article

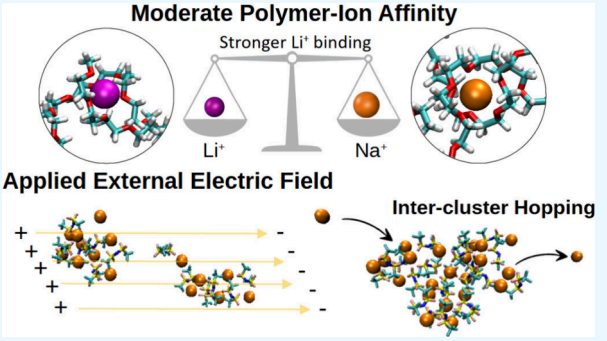
Role of Ion Interactions in Molecular Design Rules for Li^+ and Na^+ Solid Polymer Electrolytes

Gabriela Campos-Fernández,* Patricia Pérez, Eduardo Chamorro, and Fernando González-Nilo

Cite This: *ACS Appl. Polym. Mater.* 2026, 8, 4682−4692 Read Online

ACCESS | Metrics & More | Article Recommendations | Supporting Information

ABSTRACT: Solid polymer electrolytes (SPEs) are promising candidates for next-generation all-solid-state batteries owing to their safety and mechanical flexibility; however, their low ionic conductivity remains a significant bottleneck. In this work, atomistic molecular dynamics simulations systematically elucidated how polymer chemistry governs the transport mechanisms of Li^+ and Na^+ ions in chemically diverse host matrices using bis(trifluoromethanesulfonyl)imide ($TFSI^-$) as a common counterion. Six representative host matrices were analyzed, featuring ether- and carbonyl-oxygen (poly(ethylene oxide) (PEO), poly(ethylene carbonate) (PEC), and poly(propylene carbonate) (PPC)), nitrile (polyacrylonitrile (PAN)), halogenated (poly(vinylidene fluoride) (PVDF), poly(vinyl chloride) (PVC)) functional groups. These functional groups were studied under external electric fields to evaluate field-driven migration. Furthermore, the glass transition temperature (T_g), radial distribution function (RDF), and free-energy were calculated to elucidate the correlation between polymer segmental dynamics, ion-solvation stability, and the resulting ionic mobility across the different functional groups. The results demonstrate that PEO and PAN facilitate efficient, polymer-mediated conduction pathways by promoting extensive salt dissociation. Instead, halogenated polymers like PVC and PVDF favor an intercluster hopping mechanism within aggregated ionic structures. The high charge density of lithium ions results in rigid coordination shells, restricting their translational motion. Conversely, sodium ions exhibit weaker binding affinities, enabling superior field-responsive mobility. This phenomenon is particularly pronounced in PVDF, where the Na^+ diffusion coefficient increases by 2 orders of magnitude under an applied electric field (from 6.4×10^{-8} to 2.1×10^{-6} cm^2/s), significantly outperforming the modest increase observed for Li^+ (from 9.2×10^{-8} to 3.7×10^{-7} cm^2/s). Free-energy analyses further confirm that Li^+ is strongly stabilized in oxygen- and nitrogen-rich environments, whereas Na^+ transport benefits from moderate polymer affinity and a more flexible coordination shell. These findings establish fundamental molecular design rules linking polymer functionality, solvation shell dynamics, and field-driven transport. This study provides a theoretical framework for the rational design of polymer hosts optimized for high-rate cation conduction in solid-state energy storage devices.

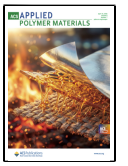


KEYWORDS: *solid polymer electrolytes, ionic conductivity, ion transport, molecular dynamics, energy materials, solvation structure*

INTRODUCTION

Developing solid polymer electrolytes (SPEs) that deliver practical room-temperature conductivity remains a central challenge for high-performance rechargeable batteries. Polymer-based electrolytes offer attractive advantages over inorganic counterparts, including ease of processability, mechanical compliance, and the ability to form stable interfaces with electrode.[1−3] Furthermore, SPEs are often regarded as a safer alternative to liquid counterparts because their mechanical properties that inhibit dendrite formation.[1,2] However, their safety profile compared to ceramic electrolytes is nuanced. While SPEs generally exhibit superior initial chemical compatibility and safety compared to sulfide-based electrolytes, particularly due to the absence of toxic SO_2 emissions and combustion behavior under thermal abuse, their primary disadvantage relative to oxide-based electrolytes is not mechanical failure, but rather their limited oxidative stability and low ionic conductivity.[3] In reality, oxide electrolytes are more susceptible to mechanical fracture and brittleness, whereas polymer electrolytes provide superior flexibility and better interfacial contact.[3] Despite these advantages, the widespread implementation of SPEs remains hindered by their limited ionic transport at ambient conditions, motivating a deeper understanding of the molecular factors governing ion−polymer interactions.[1,4−10]

Received: November 28, 2025
Revised: March 2, 2026
Accepted: March 5, 2026
Published: March 18, 2026



Downloaded from http://pubs.acs.org/aapmcd/article-pdf/8/7/4682/6749290/ap5c04495.pdf by UNIV ANDRES BELLO user on 06 August 2026

© 2026 American Chemical Society

https://doi.org/10.1021/acsapm.5c04495
ACS Appl. Polym. Mater. 2026, 8, 4682−4692

Ion transport mechanism in SPEs is intrinsically temperature-dependent and fundamentally coupled to the segmental relaxation of the polymer backbone.[11−13] In the amorphous phase, where transport predominantly occurs, cations migrate through a series of intra- and interchain hopping events facilitated by the segmental mobility above the glass transition temperature (T_g).[14,15] While ionic conductivity is often approximated by Arrhenius behavior, this description frequently fails to capture the complex dynamics of polymer electrolytes, where transport is governed by cooperative backbone relaxation. Instead, the Vogel−Fulcher−Tammann (VFT) framework better captures this behavior by explicitly accounting for the coupled motion between the ions and the polymer segments.[13,14,16] Atomistic molecular dynamics (MD) simulations naturally capture these relaxation processes and provide microscopic insight into ion migration that remains inaccessible to conventional conductivity measurements.

Poly(ethylene oxide) (PEO) remains the most studied matrix due to its ability to facilitate these hopping events through its flexible backbone; however, its semicrystalline nature at room temperature significantly limits practical performance.[17] In contrast, poly(ethylene carbonate) (PEC) and poly(propylene carbonate) (PPC) have emerged as amorphous alternatives. Their distorted, *gauche*-rich conformations frustrate chain packing and stabilize the amorphous state.[18−23] Although ester and carbonyl functionalities promote efficient salt dissociation, the inherent rigidity of these backbones, often manifested as elevated T_g values, ultimately suppresses ionic conductivity compared with PEO. This behavior highlights the fundamental competition between the thermodynamic drive for strong solvation and the kinetic requirement for rapid segmental dynamics.[15]

Numerous experimental strategies have been developed to mitigate these limitations, including the incorporation of plasticizers, nanofillers, and the design of composite or gel polymer electrolyte.[1,11,14,24] Ultimately, the challenge in molecular design lies in either enhancing this segmental coupling or successfully decoupling ion migration from the polymer dynamics, a balance that depends intimately on the specific ion-polymer coordination environment.[25] For instance, the use of plasticizers such as glycerin and the development of gel polymer electrolytes have been shown to effectively increase free volume and ionic mobility by disrupting polymer crystallinity.[26−28] Furthermore, the integration of nanofillers, such as silver nanoparticles and carbon nanotubes, as well as additives like ionic liquids, has been extensively explored to establish alternative transport pathways and improve interfacial bonding within the matrix.[11,29−32] While these strategies offer significant macroscopic improvements in conductivity and stability, a molecular-level understanding of ion transport and molecular interactions remains essential. This knowledge enables the design of polymer hosts with inherently optimized transport properties, potentially bypassing the need for conductivity-enhancing additives by addressing the fundamental mechanisms of ion migration.

Despite the growing interest in alternative chemistries, systematic comparisons of Li^+ and Na^+ transport across diverse polymer hosts remain scarce. Since similar optimization strategies are often applied to both lithium and sodium systems, a fundamental understanding of how different polymer backbones coordinate with these specific cations is required.[2,5,33,34] Recent studies have highlighted that cation chemistry and polymer molecular weight play a critical role in defining the transport mechanism; for instance, while smaller Li^+ ions may exhibit higher mobility in high-molecular-weight matrices where hopping dominates, larger Na^+ ions can surpass them in low-molecular-weight environments through different diffusion dynamics.[35] To bridge this gap, the present study investigates six representative matrices featuring distinct coordination environments: ether- and carbonyl-based oxygens (PEO, PEC, PPC), nitrile groups (polyacrylonitrile (PAN)), and weakly coordinating halogenated backbones (poly(vinyl chloride) (PVC), poly(vinylidene fluoride) (PVDF)). This selection spans a broad spectrum of solvation pathways, from high-affinity oxygen and nitrogen sites to low-affinity environments, allowing us to isolate how polymer chemistry dictates the competition between ion−ion and ion−polymer interactions. To focus specifically on cation effects, bis(trifluoromethanesulfonyl)-imide ($TFSI^-$) was chosen as the common counterion, consistent with its high degree of dissociation and widespread use in polymer electrolyte research.[36−39]

Here, Li^+ and Na^+ transport in the amorphous phases of chemically distinct polymer hosts is interrogated using atomistic MD simulations. The present study systematically evaluated glass transition temperatures (T_g), solvation thermodynamics via Free Energy Perturbation (FEP), and transport properties under both equilibrium and external electric field conditions. Operation within the linear-response regime enables accelerated exploration of ionic mobility without perturbing the fundamental structural integrity of the polymer matrix.

The simulated systems are constructed as idealized short-chain polymer models, allowing precise characterization of local coordination environments while avoiding the complexity of long-range entanglements. Although simplified compared with high-molecular-weight systems, these models isolate the chemical determinants of transport, namely solvation stability, coordination dynamics, and segmental flexibility, providing a fundamental basis for mechanistic interpretation.

By correlating functional-group chemistry with ion coordination, clustering kinetics, and field-responsive mobility, this work establishes molecular design rules that differentiate Li^+ and Na^+ transport in solid polymer electrolytes focusing on ion interactions. These results bridge macroscopic experimental strategies and microscopic transport mechanisms, providing a predictive framework for the rational design of polymer hosts tailored to specific charge carriers in next-generation solid-state energy storage devices.

COMPUTATIONAL DETAILS

All molecular dynamics (MD) simulations used the GROMACS software with the OPLS2005 force field. The simulated systems consisted of 120 polymer chains, each with 40 repeat units, and 60 salt molecules (either LiTFSI or NaTFSI). This setup corresponds to a dilute-solution regime (a salt-to-monomer ratio of 1:80), which was specifically chosen to minimize ion−ion interactions and prioritize the characterization of fundamental cation−polymer coordination. The polymer hosts investigated were PEO, PEC, PPC, PAN, PVDF, and PVC. The atomic charges for all ionic species were scaled by a factor of 0.8 to incorporate effective polarizability effects. This refinement is essential to prevent the overbinding of ions to the polymer host, a common artifact in nonpolarizable force fields that can hinder the accurate calculation of diffusion coefficients.[40,41] To construct the simulation box, initial low-density configurations were generated and subsequently compressed until the density converged to a stable value.

The glass transition temperature (T_g) was first evaluated to characterize polymer−ion interactions. PEO, PEC, and PVDF systems were equilibrated for 20 ns at 500 K, whereas PPC, PVC, and PAN were equilibrated at 600 K. A simulated annealing protocol was applied using

Downloaded from http://pubs.acs.org/aapmcd/article-pdf/8/7/4682/6479299/ap5c04495.pdf by UNIV ANDRES BELLO user on 06 August 2026

https://doi.org/10.1021/acsapm.5c04495
ACS Appl. Polym. Mater. 2026, 8, 4682−4692

heating/cooling cycles at 5 ns K^{-1} between 100 and 200 K. T_g values were obtained from hyperbola fits to the temperature−density curves. For PAN, dihedral parameters were reparameterized to reproduce the experimental T_g (details provided in the Supporting Information).

After energy minimization via the steepest descent algorithm, the systems underwent multistage equilibration in both isothermal−isobaric (NPT) and canonical (NVT) ensembles, each lasting 20 ns. The system temperature was maintained constant using the V-rescaling thermostat with a time constant of 0.1 ps. Pressure was regulated at 1 atm through the C-rescale barostat, employing a time constant of 5.0 ps and an isothermal compressibility of 4.5×10^{-5} bar^{-1}. Periodic boundary conditions were applied, and a 1.2 nm cutoff was used for nonbonded interactions, with LINCS constraints applied to all hydrogen-containing bonds. A constant temperature, set to 120 K above each polymer's T_g, was strictly maintained across all simulation stages. Subsequently, NVT production runs were performed for at least 100 ns and 2 fs time step to quantify transport properties under these stable thermal conditions.

Ion binding stability was measured using Free Energy Perturbation (FEP) with the Bennett Acceptance Ratio (BAR) method, employing 20 perturbation windows (10 ns equilibrium +0.5 ns production per window). FEP calculations were conducted on both multisalt systems (~60 ion pairs) and single-ion reference systems to assess intrinsic binding free energies.

Transport properties were computed both with and without an external electric field of 0.3 V nm^{-1} along the z-axis. Ionic conductivity (σ) was calculated using the Nernst−Einstein relation:[42]

$$\sigma = \frac{n_+ q_+^{\ 2} D_+}{k_B T} + \frac{n_- q_-^{\ 2} D_-}{k_B T} \tag{1}$$

where n is the number density, q the ionic charge, D the diffusion coefficient, k_B Boltzmann's constant, and T the temperature.

Ion mobility (μ) was obtained from drift velocity (v_d) under the applied field E:

$$\mu_\pm = \frac{v_{\pm d}}{E} \tag{2}$$

and

$$D_\pm = \frac{\mu_\pm k_B T}{q_\pm} \tag{3}$$

The cation transference number (t_+)was evaluated as

$$t_+ = \frac{\sigma_+}{\sigma_+ + \sigma_-} \tag{4}$$

Self-diffusion coefficients (D_{self}) were extracted from the mean-squared displacement (MSD):

$$\mathrm{MSD}(t) = \langle |r_i(t) - r_i(t_0)|^2 \rangle \quad (E = 0) \tag{5}$$

$$\mathrm{MSD}(t) = \langle |r_i(t) - r_i(t_0) - v_d t|^2 \rangle \quad (E \neq 0) \tag{6}$$

and determined from the long-time slope:

$$D_{self} = \lim_{t \to 0} \frac{\mathrm{MSD}(t)}{2dt} \tag{7}$$

where $r_i(t)$ denotes the position of ion i at time t, and the brackets $\langle\rangle$ indicate an ensemble average over all ions and time origins, and d is the dimensionality. Reported values represent the average over three independent replicas, with error bars corresponding to one standard deviation.

RESULTS AND DISCUSSION

This section presents a systematic analysis of the molecular dynamics simulation results to compare the transport mechanisms of Li^+ and Na^+ across the different polymer hosts. Initial focus is placed on fundamental structural and dynamical properties, such as the glass transition temperature (T_g) and solvation environments, which reveal the intrinsic stabilization differences between the two cations. These structural insights are subsequently linked to macroscopic transport parameters, including ionic conductivity, diffusion coefficients, and transference numbers, evaluated under both equilibrium and nonequilibrium (external electric field) conditions. Finally, ion clustering phenomena and polymer conformational responses are examined, providing an integrated framework to elucidate how specific polymer−ion interactions govern the performance of solid polymer electrolytes.

Glass Transition Temperature

The glass transition temperature (T_g) marks the change from a rigid, glassy state to a more flexible, viscoelastic regime, typically accompanied by an increase in ionic conductivity.[12,43,44] In this study, T_g was determined for both neat polymers (see Supporting Information) and polymer−salt systems. Molecular dynamics simulations systematically overpredict T_g relative to experimental benchmarks. This discrepancy is primarily attributed to the ultrahigh cooling rates required by simulation time scales—conditions that, while often inaccessible to experimental protocols, provide critical insights into polymer behavior under extreme thermodynamic paths.[43] A notable case in this work is PVDF, where a specific reparameterization of dihedral potentials was implemented to further improve the correlation between the atomistic model and experimental data (details in Supporting Information).

Differences across hosts reflected their distinct chemical architectures. PAN displayed the highest T_g values, attributed to strong dipole−dipole interactions from the nitrile groups, while PVC showed elevated T_g consistent with restricted segmental motion. In contrast, the methyl group in PPC introduced steric repulsions that increased intramolecular disorder relative to PEC. Notably, PEO and PVDF exhibited the lowest T_g values, confirming their superior chain flexibility and suitability as electrolyte hosts for low-temperature applications.

Salt incorporation led to a systematic increase in T_g across all hosts. A consistent shift was observed between salts, where Na-based systems exhibited T_g values approximately 3 K lower than those containing Li (see Figure 1). This trend aligns with recent reports on PEO-XTFSI (X = Li, Na) systems at low molecular weight regime,[36] and is attributed to the stronger electrostatic tethering provided by Li^+, which imposes greater constraints on chain relaxation. Importantly, the consistency in the polymer ranking for both salts indicates that the chemical nature of the host remains the primary determinant of the system's glass transition behavior.

Solvation Characterization and Stability

To quantify cation solvation across the different hosts, radial distribution functions (RDFs) and coordination numbers (CNs) were computed for Li^+ and Na^+ with respect to $TFSI^-$ oxygens and polymer functional groups (Figure 2). At T_g + 120 K, both cations exhibit a well-defined first solvation shell, characterized by peaks at ~ 2.1 Å for Li^+ and ~ 2.4 Å for Na^+. The absence of a distinct secondary shell suggests that ion-polymer interactions are dominated by short-range electrostatic forces. Notably, the peak intensity and distribution are strongly modulated by the specific polymer functionality; for instance, oxygen-containing groups (PEO, PEC, PPC) display sharper coordination environments compared to the nitrogen-based environment in PAN, reflecting differences in the Lewis basicity of the host's binding sites.

Downloaded from http://pubs.acs.org/aapmcd/article-pdf/8/7/4682/6479299/ap5c04495.pdf by UNIV ANDRES BELLO user on 06 August 2026

https://doi.org/10.1021/acsapm.5c04495
ACS Appl. Polym. Mater. 2026, 8, 4682−4692

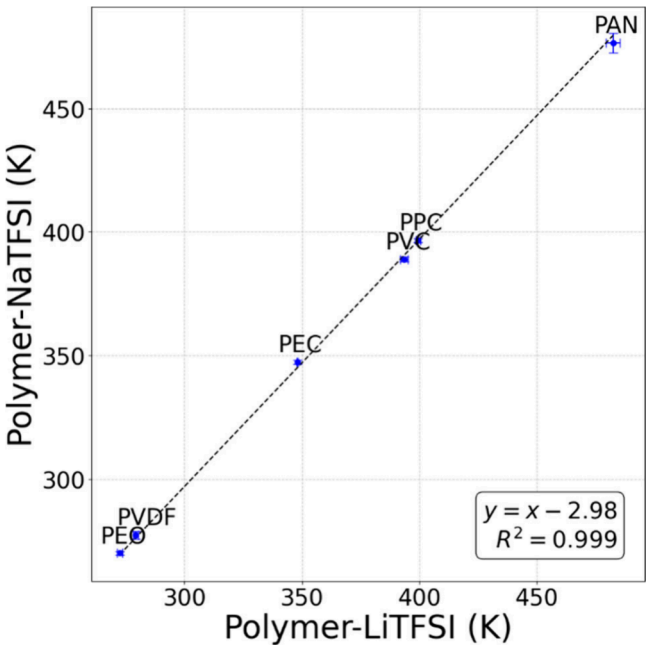


Figure 1. Relationship between the glass transition temperatures (T_g's) of polymer−salt systems containing NaTFSI and LiTFSI. Each data point represents a specific polymer host, and error bars indicate the standard deviation from three independent simulations.

Analysis of coordination numbers (CN) reveals that ether (PEO) and nitrile (PAN) groups provide a highly coordinating environment (CN ∼ 6 and 4, respectively), while Li^+−$TFSI^-$ interactions remain comparatively weak (CN < 2). This indicates a polymer-dominated solvation regime driven by the Lewis basicity of the oxygen and nitrogen lone pairs. Representative solvation motifs illustrating these distinct hosts are provided in Figure 3. In contrast, in halogenated hosts such as PVDF and PVC, the backbone contributions to the first solvation shell are minimal, and the $TFSI^-$ anion dominates the local environment (CN > 4). As evidenced by the prominent RDF peaks and the representative solvation motifs in Figure 2, this behavior suggests limited salt dissociation in halogenated matrices. In these systems, the lack of strong cation-binding sites forces the ions to remain as clusters or contact ion pairs, with a solvation shell primarily composed of $TFSI^-$ oxygens. This shift from polymer-dominated to anion-dominated solvation significantly impacts ion mobility, as the absence of strong polymer coordination in PVDF and PVC may facilitate transport mechanisms distinct from the typical ion hopping observed in PEO.

PEC and PPC exhibit a distinctive bimodal RDF, with peaks assigned to carbonyl and alkyl oxygens of the backbone. The dominant interaction involves the carbonyl oxygen, while the secondary peak reflects the extended conformation of the polymer (Figure 4). Coordination number analysis indicates 2−4 polymer oxygens per cation, typically complemented by two $TFSI^-$ oxygens, yielding mixed polymer−anion solvation shells.

Na^+ follows similar trends but with broader peaks shifted to larger distances, reflecting a more diffuse shell, larger cavity size, and weaker interactions—all consistent with its lower charge density relative to Li^+. The broader environment permits slightly higher CN, as Na^+ can engage multiple donors despite weaker pairwise interactions.

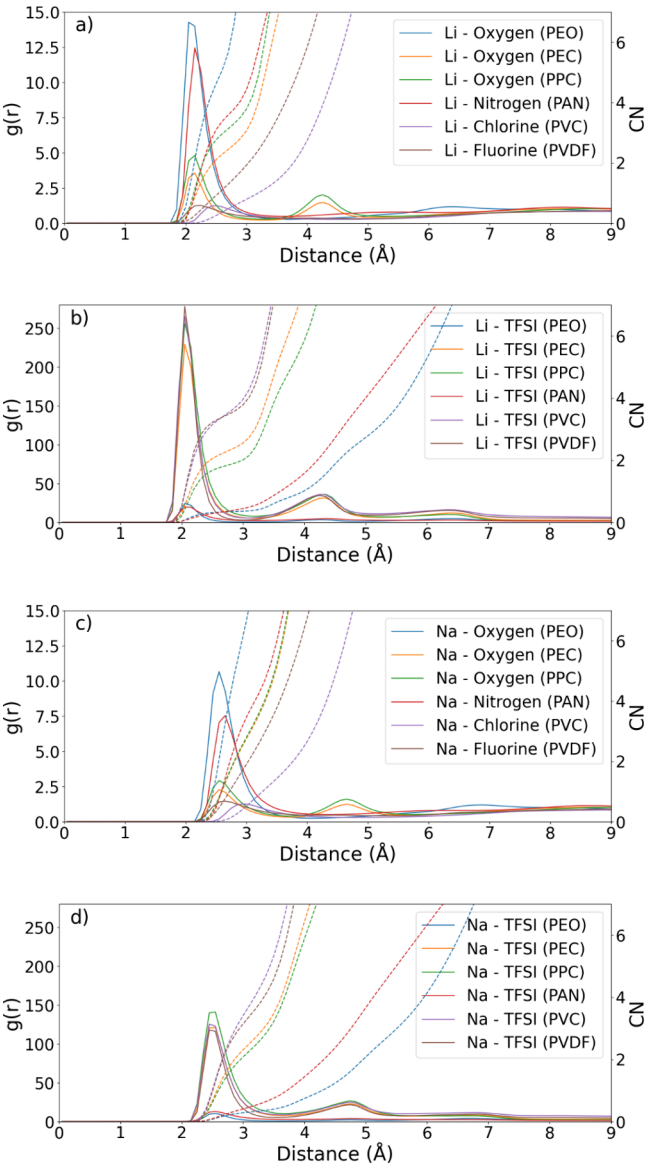


Figure 2. Radial distribution functions ($g(r)$) and cumulative coordination numbers for polymer−salt systems. (a, b) Li^+ coordination with polymer functional groups and $TFSI^-$ oxygens. (c, d) Na^+ coordination environments. Dashed lines follow the same color scheme as the solid lines.

To complement the structural analysis, free energy perturbation (FEP) was performed to evaluate the $Li^+ \rightarrow Na^+$ alchemical transformation (Table 1). Across all host matrices, the relative free energy change ($\Delta\Delta G$) remained positive, indicating a greater thermodynamic stabilization of Li^+ relative to Na^+. The higher $\Delta\Delta G$ values observed for PEO, PAN, and PEC (14.1−14.7 kcal mol^{-1}) correlate with the well-defined and rigid solvation shells formed by these groups, whose high Lewis basicity promotes a strong coordination affinity with the cationic species. Conversely, PVDF and PVC exhibited lower $\Delta\Delta G$ values (∼12.4 kcal mol^{-1}), aligning with the weaker and more diffuse polymer coordination environments previously identified. These results suggest that while Li^+ is energetically favored in all systems, the strength of this preference is significantly modulated by the ability of the polymer backbone to effectively coordinate the cation.

Downloaded from http://pubs.acs.org/aapmcd/article-pdf/8/7/4682/6479299/ap5c04495.pdf by UNIV ANDRES BELLO user on 06 August 2026

https://doi.org/10.1021/acsapm.5c04495
ACS Appl. Polym. Mater. 2026, 8, 4682−4692

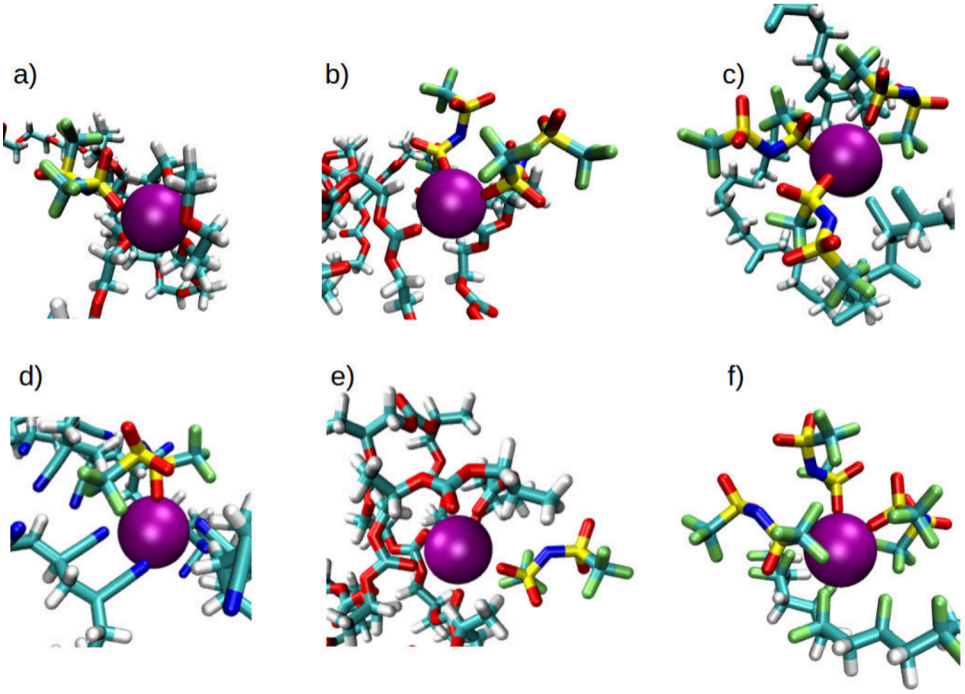


Figure 3. Representative snapshots of Li^+ coordination in polymer hosts: (a) PEO, (b) PEC, (c) PVC, (d) PAN, (e) PPC, and (f) PVDF. Lithium–polymer contacts are mediated by backbone oxygens and are especially pronounced in PVC and PVDF, where interactions occur primarily at the boundaries of ionic clusters. Similar solvation motifs were also observed in Na^+-containing systems. Atoms are represented as follows: Li in purple, O in red, C in cyan, S in yellow, H in white, and N in blue.

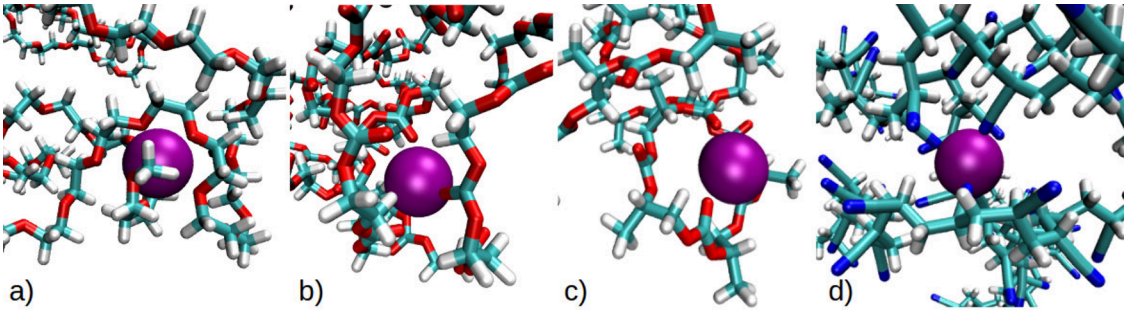


Figure 4. Representative snapshots of Li^+ fully solvated by (a) PEO, (b) PEC, (c) PPC, and (d) PAN. In PEC and PPC, Li^+ preferentially coordinates with carbonyl oxygens (red), while in PAN it exhibits 4-fold coordination by nitrile groups. Similar solvation motifs were observed for Na^+. Atoms are represented as follows: Li in purple, O in red, C in cyan, H in white, and N in blue.

Table 1. Free Energy Differences (ΔΔGs) for the Li^+ to Na^+ Alchemical Transformation in Various Polymer Environments Derived from Free Energy Perturbation (FEP) at T_g + 120 K[a]

	Temperature (K)	ΔΔG $Li^+ \rightarrow Na^+$ (kcal/mol) Average	ΔΔG $Li^+ \rightarrow Na^+$ (kcal/mol) Single-ion
PEO	391	14.63 ± 0.04	14.53 ± 0.11
PEC	468	14.38 ± 0.02	13.63 ± 0.12
PPC	518	14.10 ± 0.02	14.05 ± 0.06
PAN	600	14.68 ± 0.02	14.39 ± 0.10
PVDF	398	12.50 ± 0.02	9.87 ± 0.06
PVC	511	12.35 ± 0.01	6.62 ± 0.05

[a]Results are shown for both multi-salt (average) and single-ion pair systems.

Calculations performed at the single-ion limit (effectively removing ion clustering) further disentangle the environmental effects from the intrinsic polymer coordination. In halogenated matrices such as PVDF and PVC, $\Delta\Delta G$ decreases markedly to approximately 9.9 and 6.6 kcal mol^{-1}, respectively. This significant drop reveals that ion clustering plays a critical role in stabilizing Li^+ within these hosts, compensating for the lack of strong polymer-cation interactions. In contrast, PEO, PAN, PEC, and PPC exhibit similar $\Delta\Delta G$ values in both single-ion and multisalt systems. This consistency supports a polymer-dominated solvation mechanism that remains energetically robust regardless of ion aggregation, confirming that these functional groups possess sufficient Lewis basicity to stabilize the cations independently.

Analysis of the RDF and CN profiles confirms a pronounced Li^+–TFSI aggregation in PVC and PVDF, a result consistent with the lower $\Delta\Delta G$ values (~12.4 kcal mol^{-1}) obtained for these hosts. These findings demonstrate that the cation environment in halogenated polymers is predominantly

https://doi.org/10.1021/acsapm.5c04495
ACS Appl. Polym. Mater. 2026, 8, 4682–4692

Downloaded from http://pubs.acs.org/aapmcd/article-pdf/8/7/4682/6749299/ap5c04495.pdf by UNIV ANDRES BELLO user on 06 August 2026

governed by anion coordination rather than direct polymer−ion interactions. As will be demonstrated in the following sections, this clustering persists even under the application of an external electric field, suggesting that ion transport in these matrices occurs via intercluster hopping rather than the conventional segmental motion assisted transport typical of more coordinating hosts like PEO.

In contrast, PEC and PPC maintain a mixed solvation regime, typically characterized by the presence of one or two $TFSI^-$ oxygens within the first coordination shell, which may hinder ion mobility (Figures 3b and 3e). Furthermore, PAN and PEO primarily solvate cations via the polymer backbone, with only occasional ion-pairing. Residence-time autocorrelation functions (Figures S5−S6) reinforce these structural trends; under an external field, cation−polymer residence times exhibit a slight increase, while cation−anion residence times decrease. Notably, the electric field more effectively disrupts cation−anion associations in Na^+ systems compared to Li^+ systems. This difference underscores the distinct roles of ion clustering in modulating transport, suggesting that Na^+ transport is more susceptible to field-induced decoupling from the anionic environment.

Ion Transport Characterization

At T_g + 120 K and under an applied electric field, ionic conductivity spans 3×10^{-6} - 4×10^{-4} S cm^{-1} for Li systems and 3×10^{-5} - 5×10^{-4} S cm^{-1} for Na systems (Figure 5). Among

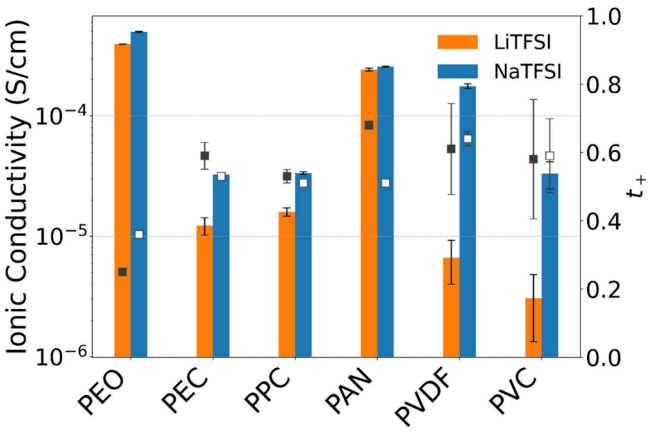


Figure 5. Ionic conductivity (σ, left axis) and cation transference numbers (t_+, right axis) for Li^+- and Na^+-based polymer electrolytes. Bars represent ionic conductivity for Li (orange) and Na (blue) systems, while points indicate t_+ values for Li (black squares) and Na (white squares). Error bars for σ and t_+ correspond to the standard deviation of block averages and propagated uncertainty, respectively.

Li^+-based systems, PEO and PAN exhibit the highest conductivities, followed by PEC and PPC. Notably, in Na^+ systems, PVDF and PVC display higher ionic conductivities than PEC and PPC, indicating a transition in the underlying transport mechanism. These trends suggest that while Li^+ mobility is constrained by strong Li^+-anion coordination, the larger Na^+ cations in PVDF and PVC environments facilitate an intercluster hopping mechanism. Unlike the behavior in coordinating hosts, transport in halogenated matrices appears largely decoupled from the polymer backbone dynamics, leveraging persistent ion aggregation to maintain macroscopic ionic flux. Consequently, these distinct solvation environments induce significant differences in transport efficiency between the two cations.

Cation transference numbers (t^+) further distinguish the underlying transport mechanisms across the host matrices (Figure 5). Na^+ exhibits higher t^+ values in PEO, PVDF, and PVC, whereas Li^+ shows higher t^+ in PEC, PPC, and PAN. Since total ionic conductivity is a function of both species' mobilities, a higher t^+ indicates a more effective cation-dominated transport regime. The behavior in PAN is particularly significant: the observed $t^+_{Li^+} > t^+_{Na^+}$ is consistent with a four-coordinate interchain pathway. This environment is characterized by prolonged cation-polymer residence times and suppressed Li−$TFSI^-$ interactions (Figures S3 and S4), which collectively promote ion-pair dissociation. In PEO, while Li^+ migration is largely governed by intrachain coordination, Na^+ exhibits shorter residence times and enhanced interchain hopping, explaining its superior conductivity. Conversely, in PEC and PPC, the cations occupy coordination sites where the polymer provides 4-fold coordination via carbonyl groups. Due to the Lewis basicity of the carbonyl oxygen compared to the ether oxygen in PEO, these sites form more localized and rigid solvation environments. This promotes an increased anionic involvement, where two $TFSI^-$ oxygens typically supplement the first solvation shell. The resulting 6-fold coordination environment correlates with the lower ionic conductivity and reduced t^+ observed in these carbonate-based hosts.

Diffusion coefficients (Figure 6) reveal that the application of an external electric field generally enhances ion diffusivity by promoting the dissociation of ion pairs and aggregations, with the PVC−Li^+ system being a notable exception. In this specific host, Li^+ diffusion is hindered by persistent and dense ion clustering, where the cations remain strongly tethered within the aggregates—a phenomenon that will be analyzed in detail in the following section. In contrast, in PEO, the high affinity between Li^+ and ether oxygens restricts the cation to localized intrachain dynamics, limiting macroscopic diffusion. Conversely, PAN provides a distinct solvation environment where the rigid backbone facilitates a 4-fold interchain coordination. This configuration results in reduced coordination strength enabling frequent hopping events, thereby significantly increasing Li^+ diffusivity compared to the PEO matrix.

The application of the electric field markedly increases ion diffusion across most systems, although the magnitude of this effect is highly ion- and host-dependent. In PEO, the field-induced enhancement is more pronounced for the TFSI- anions, whereas cation mobility increases to varying degrees in other matrices. A critical exception occurs in PVC-Li, where the field promotes the growth of large ionic aggregations that effectively hinder transport. This suggests that the local solvation environment, determined by specific polymer functional groups, is the primary determinant of ion mobility. Specifically, solvation environments characterized by moderate affinity, such as those found in PAN for Li^+,promote higher mobility compared to the overly stable coordination observed in ether-based systems. While lithium exhibits a higher affinity for ether oxygens and sodium for nitrile groups, the relative impact on transport depends on the balance between this affinity and the polymer's structural flexibility. Consequently, the distinct coordination preferences of each cation lead to significant differences in their drift velocities within the same polymeric matrix.

Conformational Analysis via Radius of Gyration

The conformational response to an applied field (0.3 V nm^{-1}) was evaluated through the components of the radius of gyration (Figure 7). All polymer hosts exhibit anisotropic deformation

Downloaded from http://pubs.acs.org/aapmcd/article-pdf/8/7/4682/6749299/ap5c04495.pdf by UNIV ANDRES BELLO user on 06 August 2026

https://doi.org/10.1021/acsapm.5c04495
ACS Appl. Polym. Mater. 2026, 8, 4682−4692

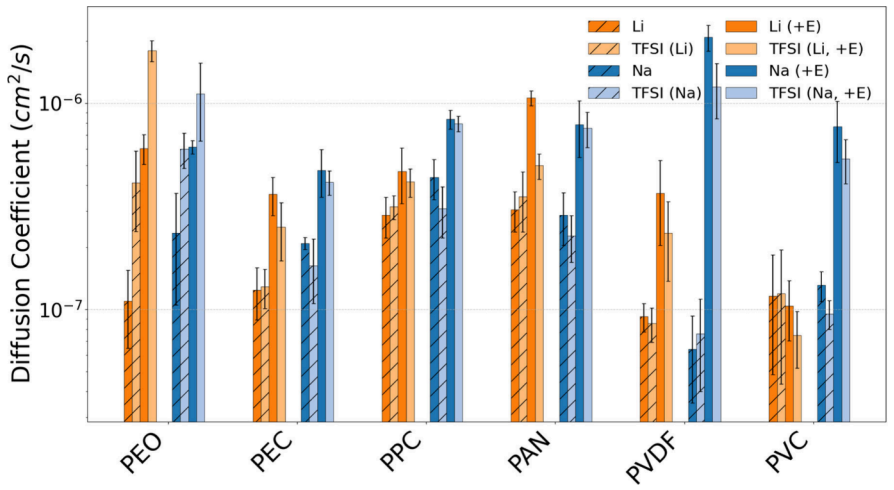


Figure 6. Diffusion coefficients for cations and anions across various polymer hosts calculated under equilibrium and applied electric field (0.3 V nm^{-1}) conditions. Li-based systems are shown in orange and Na-based systems are in blue, with corresponding $TFSI^-$ anions displayed in lighter shades of the same colors. Hatched bars represent zero-field simulations, while solid bars denote values under the applied field. Error bars indicate the standard deviation from three independent trajectories.

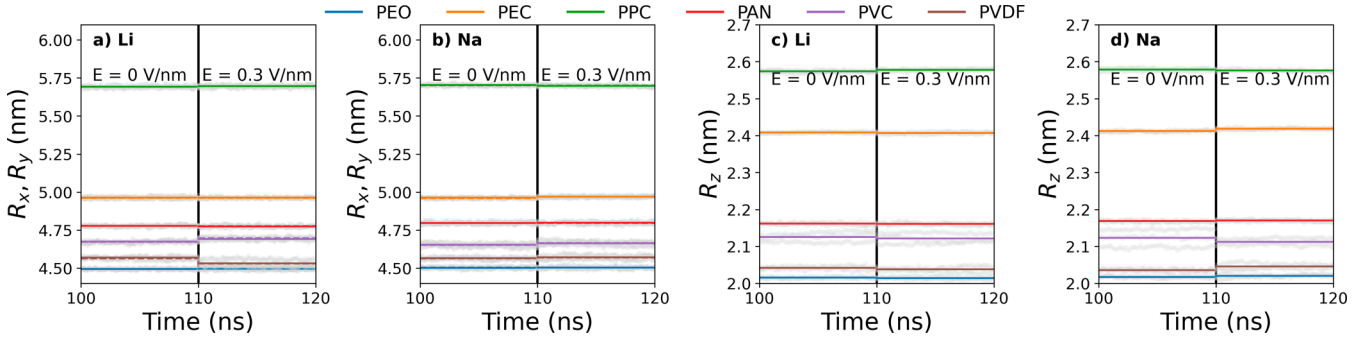


Figure 7. Radius of gyration (R_g) of polymer hosts in Li^+- and Na^+-containing systems under applied electric fields. R_x and R_y for Li^+ (a) and Na^+ (b), and R_z for Li^+ (c) and Na^+ (d). Results are shown for all six polymer hosts (PEO, PEC, PPC, PAN, PVC, and PVDF).

characterized by elongation along the field axis (increased R_z) and a corresponding compaction in the orthogonal directions (reduced R_x, R_y). Quantitatively, R_z increases to 4.5−4.7 nm, while R_x and R_y contract to 2.0−2.6 nm.

Systematic differences between Li^+ and Na^+ systems emerge from this analysis. In Li^+- based electrolytes, the electric field typically induces a moderate compaction in R_x and R_y (exception: PVC−Li, slight increase). In Na systems generally exhibit increases in both R_x and R_y (except PPC−Na), and R_z shows more pronounced elongation. While most Li^+ cases show modest R_z growth, PPC−Li and PVC−Li undergoes more significant elongation. PVDF−Na system behaves anomalously, showing a sharp R_z reduction under the field. Such behavior likely arises from the cation's drag response under the applied electric field, where the ion's movement effectively pulls and collapses the polymer backbone due to their strong coordination.

Influence of the External Electric Field on Ion Aggregation

Ion aggregation was quantified by calculating the average number of ion pairs under steady-state conditions (Figure 8). The degree of salt dissociation is highly host-dependent: PEO and PAN exhibit high dissociation levels, PEC and PPC show intermediate behavior, and PVC and PVDF display extensive aggregation. This aggregation profile reflects a delicate balance between cation−polymer affinity and cation−anion attraction, further modulated by backbone conformational constraints.

Results from single-ion system simulations support this interpretation, indicating that the polymer host's ability to coordinate the cation fundamentally dictates the extent of counterion proximity. In poorly coordinated matrices such as PVC and PVDF, the lack of effective cation shielding by the polymer chains facilitates persistent ion-pair formation and subsequent aggregation, which remains a dominant feature even under an applied field.

The applied field reveals a fundamental contrast between Li^+ and Na^+ transport mechanisms. In PVC−Li and PVDF−Li, the field drives aggregation growth, where smaller ion groups merge into larger clusters that effectively impede long-range transport. In sharp contrast, the field destabilizes these structures in Na^+ systems, promoting field-induced fragmentation of the aggregates. This process enhances diffusion of both Na^+ and $TFSI^-$ by reducing the average size of ion groupings. This behavior accounts for the notably higher diffusion coefficients observed in sodium-based electrolytes, where weaker electrostatic interactions allow the electric field to more easily disrupt and break apart the ionic aggregations.

Notably, while the electric field induces slight conformational changes in the polymer chains (as evidenced by R_g analysis), it does not significantly alter the local primary coordination environment; instead, it predominantly modulates the dynamics of the ion aggregates. Although high levels of aggregation typically limit individual ion mobility, macroscopic transport is

https://doi.org/10.1021/acsapm.5c04495
ACS Appl. Polym. Mater. 2026, 8, 4682−4692

Downloaded from http://pubs.acs.org/aapmcd/article-pdf/8/7/4682/6479299/ap5c04495.pdf by UNIV ANDRES BELLO user on 06 August 2026

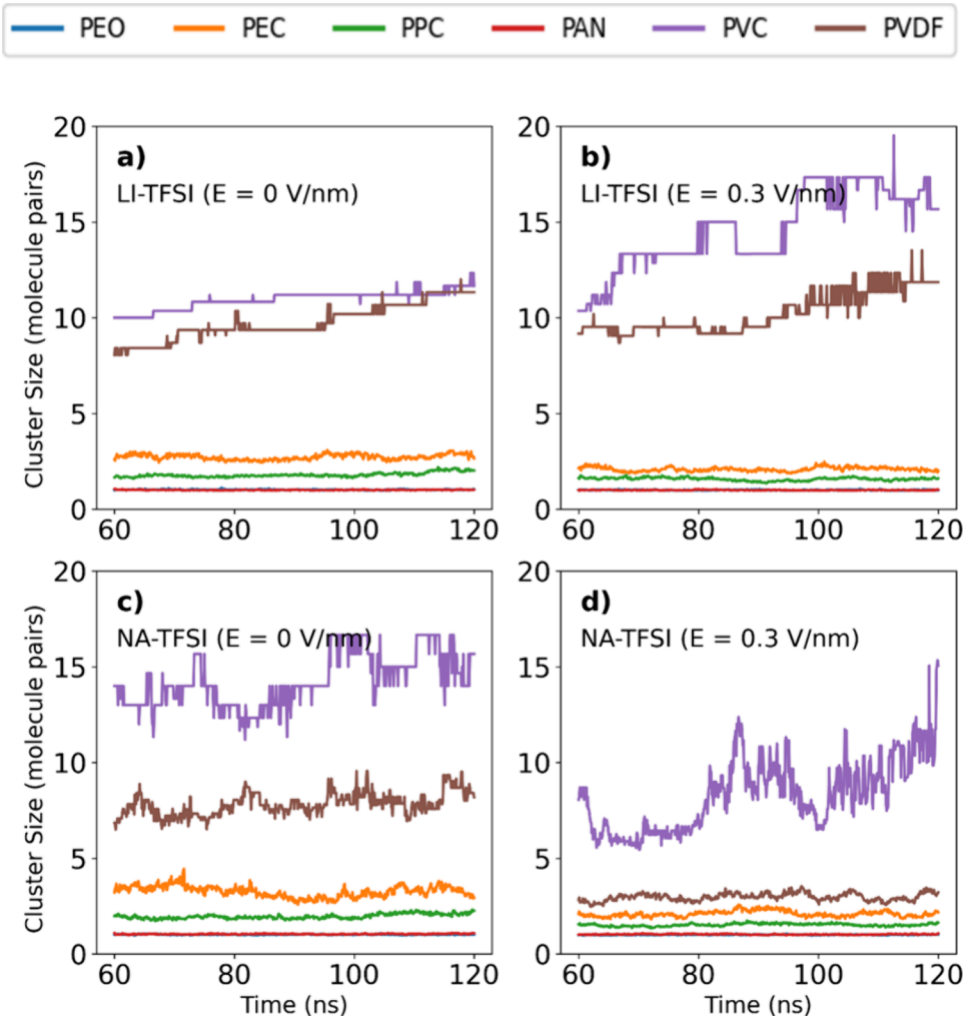


Figure 8. Cluster size evolution for different polymer hosts in Li^+−TFSI (a, b) and Na^+−TFSI (c, d) systems with (b, d) and without (a, c) an applied electric field (E = 0.3 V/nm). Each trace corresponds to a different polymer host (PEO, PEC, PPC, PAN, PVC, PVDF). While most polymers exhibit small and stable clusters, PVC and PVDF systems display pronounced aggregation. Under an applied electric field, Li^+-based systems (b) show further cluster growth, whereas Na^+-based systems (d) undergo partial disaggregation, leading to smaller and more dynamic clusters. This contrasting field response highlights the stronger ion−polymer affinity and clustering tendency of lithium compared to sodium.

maintained via an intercluster hopping mechanism. In this process, cations undergo rapid exchange between adjacent ion aggregates. This alternative conduction pathway explains the relatively high conductivity and diffusion coefficients observed in highly aggregated hosts, particularly for Na^+ in PVC and PVDF. The more prominent increase in LiTFSI cluster size in PVC compared to PVDF is directly linked to the lower intrinsic stabilizing capacity of the PVC backbone ($\Delta\Delta G \sim 6.6$ kcal/mol). This lack of competitive polymer-ion coordination forces a stronger reliance on anion-mediated stabilization, leading to the formation of larger ionic aggregates that persist even under external electric fields.

Quantitative analysis confirms these trends. In PVC, the average Li^+ aggregation size increases from approximately 11 to 16 ion pairs under the field, whereas Na^+ aggregates decrease from 15 to 10. A more dramatic shift occurs in PVDF, where Li^+ aggregations remain nearly stagnant (shifting from 10 to 11), while Na^+ aggregates shrink significantly from 7 to 3. This field-induced reduction in aggregate size is highly consistent with the superior conductivity measured in the Na−PVDF system. Visual inspection (Figure 9) of a Li^+ aggregate in PVDF reveals the cation residing at the periphery with minimal backbone contact, further corroborating the RDF and CN analyses.

Overall, these results reveal that ion transport in solid polymer electrolytes arises from a delicate interplay between polymer functionality, solvation thermodynamics, and dynamic response to external driving forces. The systematic trends observed across chemically distinct hosts demonstrate that neither strong coordination nor weak binding alone guarantees optimal transport; instead, mobility is maximized within an intermediate regime where polymer−ion interactions provide sufficient stabilization while preserving rapid detachment and structural flexibility. The application of an electric field further exposes fundamental differences between Li^+ and Na^+, highlighting how cation identity modulates cluster stability, dissociation kinetics, and migration pathways. By unifying structural descriptors, free-energy stabilization, clustering behavior, and field-driven dynamics within a consistent atomistic framework, the present study establishes a mechanistic basis for identifying transferable molecular design principles. These insights form the foundation for the general conclusions presented below and provide a rational framework for the targeted engineering of polymer electrolytes with tailored transport properties.

https://doi.org/10.1021/acsapm.5c04495
ACS Appl. Polym. Mater. 2026, 8, 4682−4692

Downloaded from http://pubs.acs.org/aapmcd/article-pdf/8/7/4682/6749299/ap5c04495.pdf by UNIV ANDRES BELLO user on 06 August 2026

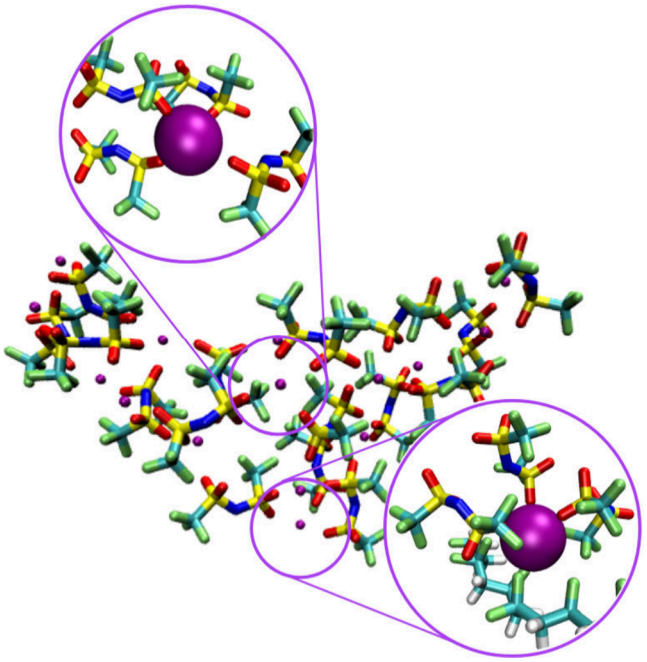


Figure 9. Representative snapshot of a Li^+−TFSI cluster in poly(vinylidene fluoride) (PVDF). Lithium ions (purple) are primarily coordinated by TFSI anions (yellow/red/blue/cyan/green atoms) while maintaining only peripheral contact with the PVDF backbone (cyan/green atoms). This morphology reflects the limited role of the polymer in cation solvation and the dominance of anion-driven coordination. A similar aggregation pattern is observed in poly(vinyl chloride) (PVC) and in sodium-based counterparts, consistent with RDF and CN analyses.

CONCLUSIONS

This study systematically characterized Li^+ and Na^+ transport in solid polymer electrolytes across a broad range of polymer chemistries under both equilibrium and applied electric field conditions. The results demonstrate that polymer chemistry is the primary determinant of solvation stability and transport behavior, with ion coordination being dominated by the first solvation shell in all cases. Ether-, carbonyl-, and nitrile-based hosts (PEO, PEC, PPC, and PAN) form well-defined polymer-mediated coordination environments, whereas halogenated matrices favor anion-dominated solvation and ionic aggregation. Beyond coordination geometry, the Lewis basicity of the functional groups emerges as a key parameter controlling ion mobility.

Across all studied hosts, Li^+ exhibits significantly stronger binding and lower mobility compared to Na^+, as confirmed by consistently positive $\Delta\Delta G$ ($Li^+ \rightarrow Na^+$) values and higher T_g. Strong Li−polymer interactions restrict segmental flexibility and suppress both diffusivity and ionic conductivity. In contrast, Na^+ benefits from weaker coordination, larger effective solvation cavities, and enhanced detachment dynamics, resulting in higher conductivity that is further amplified under applied electric fields. Importantly, the electric field more efficiently disrupts Na^+−anion associations than Li^+−anion pairs, promoting salt dissociation and facilitating drift-dominated transport.

In highly aggregated environments, these weaker electrostatic interactions enable an intercluster hopping mechanism in which cations migrate by jumping between ionic domains rather than relying exclusively on polymer segmental motion. Together, these results identify a central molecular design principle: optimal ion transport arises from a moderate polymer−ion affinity—strong enough to ensure solvation stability, yet sufficiently labile to permit rapid detachment and migration. By establishing this coordination-based design rule, this work provides a predictive framework for tailoring polymer electrolytes and highlights sodium-based systems as particularly promising candidates for high-rate solid-state energy storage at near-ambient temperatures.

ASSOCIATED CONTENT

Supporting Information

The Supporting Information is available free of charge at https://pubs.acs.org/doi/10.1021/acsapm.5c04495.

Chemical structures of all simulated polymer hosts; comparison tables of theoretical and experimental glass transition temperatures for model validation; detailed methodology and plots for the reparameterization of PVDF dihedral angles; autocorrelation function analysis (PDF)

AUTHOR INFORMATION

Corresponding Author

Gabriela Campos-Fernández − *Doctorado en Fisicoquímica Molecular, Facultad de Ciencias Exactas, Universidad Andrés Bello, Santiago 8370146, Chile; Center for Bioinformatics and Integrative Biology (CBIB), Facultad de Ciencias de la Vida, Universidad Andrés Bello, Santiago 8370035, Chile;* orcid.org/0000-0001-7107-227X; Email: m.camposfernandez@uandresbello.edu

Authors

Patricia Pérez − *Facultad de Ciencias, Escuela de Química y Farmacia, Universidad San Sebastián, Huechuraba, Santiago 8580704, Chile;* orcid.org/0000-0002-6920-703X

Eduardo Chamorro − *Facultad de Ciencias, Escuela de Química y Farmacia, Universidad San Sebastián, Huechuraba, Santiago 8580704, Chile;* orcid.org/0000-0002-9200-9859

Fernando González-Nilo − *Center for Bioinformatics and Integrative Biology (CBIB), Facultad de Ciencias de la Vida, Universidad Andrés Bello, Santiago 8370035, Chile;* orcid.org/0000-0001-6857-3575

Complete contact information is available at: https://pubs.acs.org/10.1021/acsapm.5c04495

Author Contributions

Gabriela Campos-Fernández: Conceptualization, Methodology, Software, Formal Analysis, Investigation, Writing−Original Draft, Visualization, Writing−Review & Editing. **Patricia Pérez**, **Eduardo Chamorro**, and **Fernando González-Nilo**: Supervision, Funding acquisition, Writing−Review & Editing.

Notes

The authors declare no competing financial interest.

ACKNOWLEDGMENTS

The authors gratefully acknowledge financial support from the Agencia Nacional de Investigación y Desarrollo (ANID), Chile, through Doctoral Scholarship 21240328 (G.C.-F.), as well as a Fondecyt project Nos. 1221383 (P.P.) and 1231018 (E.C.).

Downloaded from http://pubs.acs.org/aapmcd/article-pdf/8/7/4682/6479299/ap5c04495.pdf by UNIV ANDRES BELLO user on 06 August 2026

This work was supported by the U.S. Army Combat Capabilities Development Command Soldier Center under Prime Contract FA807518D0014 and Delivery Order FA807522F0018 (F.G.-N.). The authors also thank Universidad Andrés Bello for providing access to the high-performance computing facilities used in this work.

REFERENCES

(1) Zhang, S.; Ma, J.; Dong, S.; Cui, G. Designing All-Solid-State Batteries by Theoretical Computation: A Review. *Electrochemical Energy Reviews* **2023**, *6* (1), 1−40.
(2) Wang, S.; Peng, B.; Lu, J.; Jie, Y.; Li, X.; Pan, Y.; Han, Y.; Cao, R.; Xu, D.; Jiao, S. Recent Progress in Rechargeable Sodium Metal Batteries: A Review. *Chemistry−A European Journal* **2023**, *29* (3), No. e202202380.
(3) Casas-Cabanas, M.; Palacín, M. R. Challenges Ahead in the Development of Solid-State Batteries. *J. Power Sources* **2025**, *659*, 238355.
(4) Li, Z.; Fu, J.; Zhou, X.; Gui, S.; Wei, L.; Yang, H.; Li, H.; Guo, X. Ionic Conduction in Polymer-Based Solid Electrolytes. *Advanced Science* **2023**, *10* (10), 2201718.
(5) Qiao, L.; Judez, X.; Rojo, T.; Armand, M.; Zhang, H. Review—Polymer Electrolytes for Sodium Batteries. *J. Electrochem. Soc.* **2020**, *167* (7), 070534.
(6) Ngai, K. S.; Ramesh, S.; Ramesh, K.; Juan, J. C. A Review of Polymer Electrolytes: Fundamental, Approaches and Applications. *Ionics* **2016**, *22* (8), 1259−1279.
(7) Goodenough, J. B.; Kim, Y. Challenges for Rechargeable Li Batteries. *Chem. Mater.* **2010**, *22* (3), 587−603.
(8) Li, Q.; Chen, J.; Fan, L.; Kong, X.; Lu, Y. Progress in Electrolytes for Rechargeable Li-Based Batteries and Beyond. *Green Energy & Environment* **2016**, *1* (1), 18−42.
(9) Sequeira, C.; Santos, D. *Polymer Electrolytes: Fundamentals and Applications*; Elsevier Ltd., 2010; DOI: 10.1533/9781845699772.1.219.
(10) Ding, Z.; Li, J.; Li, J.; An, C. Review—Interfaces: Key Issue to Be Solved for All Solid-State Lithium Battery Technologies. *J. Electrochem. Soc.* **2020**, *167* (7), 070541.
(11) Lopez, J.; Mackanic, D. G.; Cui, Y.; Bao, Z. Designing Polymers for Advanced Battery Chemistries. *Nat. Rev. Mater.* **2019**, *4* (5), 312−330.
(12) Gebert, F.; Knott, J.; Gorkin, R.; Chou, S. L.; Dou, S. X. Polymer Electrolytes for Sodium-Ion Batteries. *Energy Storage Mater.* **2021**, *36*, 10−30.
(13) Majeed, M. K.; Iqbal, R.; Ashfaq, M. Z.; Akram, M.; Majeed, M. U.; Saleem, A. Advancing All-Solid Polymer Electrolytes for Lithium Batteries: From Molecular Design to Device Integration. *Energy Storage Mater.* **2026**, *86*, 104831.
(14) Ratner, M. A.; Johansson, P.; Shriver, D. F. Polymer Electrolytes: Ionic Transport Mechanisms and Relaxation Coupling. *MRS Bull.* **2000**, *25* (3), 31−37.
(15) Mindemark, J.; Lacey, M. J.; Bowden, T.; Brandell, D. Beyond PEO—Alternative Host Materials for Li+-Conducting Solid Polymer Electrolytes. *Prog. Polym. Sci.* **2018**, *81*, 114−143.
(16) Aziz, S. B.; Woo, T. J.; Kadir, M. F. Z.; Ahmed, H. M. A Conceptual Review on Polymer Electrolytes and Ion Transport Models. *Journal of Science: Advanced Materials and Devices* **2018**, *3* (1), 1−17.
(17) Zhou, D.; Shanmukaraj, D.; Tkacheva, A.; Armand, M.; Wang, G. Polymer Electrolytes for Lithium-Based Batteries: Advances and Prospects. *Chem.* **2019**, *5* (9), 2326−2352.
(18) Sasanuma, Y.; Takahashi, Y. Structure-Property Relationships of Poly(Ethylene Carbonate) and Poly(Propylene Carbonate). *ACS Omega* **2017**, *2* (8), 4808−4819.
(19) Udipi, K.; Gillham, J. K. Poly(Ethylene Carbonate) and Poly(Propylene Carbonate): Transitions and Thermomechanical Spectra. *J. Appl. Polym. Sci.* **1974**, *18* (5), 1575−1580.
(20) Kimura, K.; Motomatsu, J.; Tominaga, Y. Correlation between Solvation Structure and Ion-Conductive Behavior of Concentrated Poly(Ethylene Carbonate)-Based Electrolytes. *J. Phys. Chem. C* **2016**, *120* (23), 12385−12391.
(21) Zhang, J.; Zhao, J.; Yue, L.; Wang, Q.; Chai, J.; Liu, Z.; Zhou, X.; Li, H.; Guo, Y.; Cui, G.; Chen, L. Safety-Reinforced Poly(Propylene Carbonate)-Based All-Solid-State Polymer Electrolyte for Ambient-Temperature Solid Polymer Lithium Batteries. *Adv. Energy Mater.* **2015**, *5* (24), 1501082.
(22) Meabe, L.; Huynh, T. V.; Lago, N.; Sardon, H.; Li, C.; O'Dell, L. A.; Armand, M.; Forsyth, M.; Mecerreyes, D. Poly(Ethylene Oxide Carbonates) Solid Polymer Electrolytes for Lithium Batteries. *Electrochim. Acta* **2018**, *264*, 367−375.
(23) Yue, H.; Li, J.; Wang, Q.; Li, C.; Zhang, J.; Li, Q.; Li, X.; Zhang, H.; Yang, S. Sandwich-Like Poly(Propylene Carbonate)-Based Electrolyte for Ambient-Temperature Solid-State Lithium Ion Batteries. *ACS Sustain. Chem. Eng.* **2018**, *6* (1), 268−274.
(24) Webb, M. A.; Jung, Y.; Pesko, D. M.; Savoie, B. M.; Yamamoto, U.; Coates, G. W.; Balsara, N. P.; Wang, Z. G.; Miller, T. F. Systematic Computational and Experimental Investigation of Lithium-Ion Transport Mechanisms in Polyester-Based Polymer Electrolytes. *ACS Cent. Sci.* **2015**, *1* (4), 198−205.
(25) Song, Z.; Chen, F.; Martinez-Ibañez, M.; Feng, W.; Forsyth, M.; Zhou, Z.; Armand, M.; Zhang, H. A Reflection on Polymer Electrolytes for Solid-State Lithium Metal Batteries. *Nat. Commun.* **2023**, *14* (1), 1−13.
(26) Mahmood, R. Y.; Kareem, A. A.; Polu, A. R. Enhancement of Ionic Conductivity and Electrochemical Stability of PVA/HPMC/PANI/CuSO4 Gel Polymer for Rechargeable Batteries Electrolytes. *Solid State Ion* **2024**, *408*, 116511.
(27) Ali, N. M.; Kareem, A. A.; Polu, A. R. Effect of Glycerin on Electrical and Thermal Properties of PVA/Copper Sulphate Gel Polymer Electrolytes. *Journal of Inorganic and Organometallic Polymers and Materials* **2022**, *32* (10), 4070−4076.
(28) Ali, N. M.; Kareem, A. A. Ionic Conductivity Enhancement for PVA/ 20wt.% CuSO4 Gel Polymer Electrolyte by Using Glycerin. *Chalcogenide Letters* **2022**, *19* (3), 217−225.
(29) Polu, A. R.; Kareem, A. A.; Rasheed, H. K. Thermal, Electrical and Electrochemical Properties of Ionic Liquid-Doped Poly(Ethylene Oxide)−LiTDI Polymer Electrolytes for Li-Ion Batteries. *J. Solid State Electrochem.* **2023**, *27* (2), 409−416.
(30) Kareem, A. A.; Polu, A. R.; Rasheed, H. K.; Alomayri, T. Effect of Silver Nanoparticles on Structural, Thermal, Electrical, and Mechanical Properties of Poly(Vinyl Alcohol) Polymer Nanocomposites. *Polym. Compos.* **2023**, *44* (6), 3281−3287.
(31) Croce, F.; Persi, L. L.; Scrosati, B.; Serraino-Fiory, F.; Plichta, E.; Hendrickson, M. A. Role of the Ceramic Fillers in Enhancing the Transport Properties of Composite Polymer Electrolytes. *Electrochim. Acta* **2001**, *46* (16), 2457−2461.
(32) Kareem, A. A. Enhanced Thermal and Electrical Properties of Epoxy/Carbon Fiber−Silicon Carbide Composites. *Advanced Composites Letters* **2020**, 29.
(33) Xiang, X.; Zhang, K.; Chen, J. Recent Advances and Prospects of Cathode Materials for Sodium-Ion Batteries. *Adv. Mater.* **2015**, *27* (36), 5343−5364.
(34) Hegde, S.; Ravindrachary, V.; Sanjeev, G.; Ismayil. Characterization and Charge Transport Properties of Sodium Ion Conducting PEO:NaBr Solid Polymer Electrolyte Films. *Polym. Eng. Sci.* **2023**, *63* (8), 2468−2483.
(35) Papamichail, C.; Techlemtzi, O.; Nikolakakou, G.; Glynos, E. Cation Chemistry and Molecular Weight Effects on the Ion Conductivity in PEO-Based Electrolytes. *ACS Macro Lett.* **2025**, *14* (2), 225−230.
(36) Papamichail, C.; Techlemtzi, O.; Nikolakakou, G.; Glynos, E. Cation Chemistry and Molecular Weight Effects on the Ion Conductivity in PEO-Based Electrolytes. *ACS Macro Lett.* **2025**, *14* (2), 225−230.

Downloaded from http://pubs.acs.org/aapmcd/article-pdf/8/7/4682/6479299/ap5c04495.pdf by UNIV ANDRES BELLO user on 06 August 2026

(37) Boschin, A.; Johansson, P. Characterization of NaX (X: TFSI, FSI) − PEO Based Solid Polymer Electrolytes for Sodium Batteries. *Electrochim. Acta* **2015**, *175*, 124−133.
(38) Kubisiak, P.; Wróbel, P.; Eilmes, A. Molecular Dynamics Investigation of Correlations in Ion Transport in MeTFSI/EMIM-TFSI (Me = Li, Na) Electrolytes. *J. Phys. Chem. B* **2020**, *124* (2), 413−421.
(39) Tominaga, Y.; Yamazaki, K.; Nanthana, V. Effect of Anions on Lithium Ion Conduction in Poly(Ethylene Carbonate)-Based Polymer Electrolytes. *J. Electrochem. Soc.* **2015**, *162* (2), A3133.
(40) Sundararaman, S.; Halat, D. M.; Reimer, J. A.; Balsara, N. P.; Prendergast, D. Understanding the Impact of Multi-Chain Ion Coordination in Poly(Ether-Acetal) Electrolytes. *Macromolecules* **2022**, *55* (21), 9880−9889.
(41) Sundararaman, S.; Halat, D. M.; Choo, Y.; Snyder, R. L.; Abel, B. A.; Coates, G. W.; Reimer, J. A.; Balsara, N. P.; Prendergast, D. Exploring the Ion Solvation Environments in Solid-State Polymer Electrolytes through Free-Energy Sampling. *Macromolecules* **2021**, *54* (18), 8590−8600.
(42) Verma, A. K.; Thorat, A. S.; Shah, J. K. Estimating Ionic Conductivity of Ionic Liquids: Nernst−Einstein and Einstein Formalisms. *Journal of Ionic Liquids* **2024**, *4* (1), 100089.
(43) Nkepsu Mbitou, R. L.; Bedoui, F. A Review on All-Atom Force Fields Capabilities to Predict Polymer Properties: Case of Poly(Methyl Methacrylate) and Polyisobutylene Polymer Systems. *Comput. Mater. Sci.* **2025**, *253*, 113861.
(44) Szczęsna-Chrzan, A.; Marczewski, M.; Syzdek, J.; Kochaniec, M. K.; Smoliński, M.; Marcinek, M. Lithium Polymer Electrolytes for Novel Batteries Application: The Review Perspective. *Appl. Phys. A: Mater. Sci. Process.* **2023**, *129* (1), 1−20.

Downloaded from http://pubs.acs.org/aapmcd/article-pdf/8/7/4682/6749299/ap5c04495.pdf by UNIV ANDRES BELLO user on 06 August 2026

https://doi.org/10.1021/acsapm.5c04495
ACS Appl. Polym. Mater. 2026, 8, 4682−4692